Anisotropic Motion of the Steroid Ring System of Cholesteryl Esters. Calculation of Carbon-13 Nuclear Magnetic Resonance Relaxation Times and Nuclear Overhauser Enhancements and Comparison with Experiment†

Daniel M. Quinn*

ABSTRACT: A quantitative model for the molecular dynamics of the steroid fused ring system of cholesteryl esters is discussed. The model describes rotational diffusive motion of the steroid rings as that of axially symmetric prolate ellipsoids and is used to generate predictions for the dependence of carbon-13 nuclear magnetic resonance (^{13}C NMR) line widths, spin–lattice relaxation times, and nuclear Overhauser enhancements of C3 and C6 of cholesteryl esters on the correlation times for rotation about the symmetry axis and about the nonunique axes of the ellipse by using the spectral density functions developed by Woessner [Woessner, D. E. (1962) *J. Chem. Phys. 37*, 647–654]. The predictions are used to calculate correlation times for motion of the steroid rings of isotropic liquid-phase cholesteryl linoleate and cholesteryl oleate from NMR spectra at magnetic field strengths of 2.35 and 6.34 T and at various temperatures. Such calculations characterize steroid ring motion of cholesteryl esters as highly anisotropic, with motion about the symmetry axis 40–130 times faster than about the nonunique axes. The fact that the line width of the C6 resonance is consistently narrower than that of C3 is attributed to the high rotational anisotropy of cholesteryl esters and to the inclination of the C6–H internuclear vector at an angle with respect to the molecular symmetry axis that is very close to the "magic angle".

Nuclear magnetic resonance spectroscopy (NMR)[1] has been frequently applied to the study of lipid-containing systems such as membranes (Gent & Prestegard, 1977) and serum lipoproteins (Kroon et al., 1982, and references cited therein) and of biomimetic neat lipid mixtures (Sears et al., 1976; Hamilton et al., 1977). The spin–lattice (T_1) and spin–spin (T_2; inversely proportional to line width) relaxation times and nuclear Overhauser enhancement (NOE) associated with the resonance of a sample nucleus contain detailed information on both the geometry of motion and rate(s) of motion(s) of the nucleus. Various authors have developed theoretical models for predicting NMR relaxation parameters of nuclei involved in isotropic (Doddrell et al., 1972) or anisotropic molecular motions (Allerhand, 1970; Allerhand et al., 1971; Doddrell et al., 1972; Woessner, 1962a,b; Wittebort & Szabo, 1978; Tancrede et al., 1978; Gent & Prestgard, 1977; Brainard & Szabo, 1981). For example, Woessner has derived equations for the T_1 and T_2 of a spin $-^1/_2$ nucleus that relaxes via homonuclear dipolar interaction and for which the dipolar interaction vector is motionally modulated by axially symmetric ellipsoidal reorientation (Woessner, 1962b). Allerhand et al. (1971) and Doddrell et al. (1972) have developed models for the dependence of T_1, T_2, and NOE on motional rate for a ^{13}C nucleus relaxing by dipolar interaction with ^{1}H and in which the ^{13}C–^{1}H internuclear vector reorients about an axis that itself is reorienting isotropically. Such a process was previously described by Woessner (1962a) for homonuclear dipolar relaxation. Yeagle (1981) has used the approaches developed by Woessner (1962a), Allerhand et al. (1971), and Doddrell et al. (1972) to characterize the anisotropic motion of cholesterol in sonicated phosphatidylcholine vesicles. His model gives a correlation time for axial rotation of cholesterol of about 10^{-10} s, with the long axis reorienting isotropically due to vesicle tumbling with a correlation time of 10^{-6} s. Brainard & Szabo (1981) assumed that motion of cholesterol in phosphatidylcholine bilayers could be described as that of an axially symmetric ellipse, with rapid and spatially unrestricted motion about the symmetry axis and spatially restricted motion about the two nonunique axes.

In this paper, the axial symmetry assumption of Brainard & Szabo (1981) and Woessner's spectral density functions (1962b) are used to calculate the dependence of T_1, line width, and NOE of C3 and C6 of cholesteryl esters on the rotational correlation times about the long and short axes of the molecule. These predictions are used herein to present a quantitative model for the motion of the steroid ring system of cholesteryl esters from ^{13}C NMR measurements on neat cholesteryl oleate and cholesteryl linoleate.

Experimental Procedures

^{13}C spectra were obtained at 6.34 T (67.89 MHz) on a Bruker HX270 spectrometer and at 2.35 T (25.14 MHz) on a Varian XL100 spectrometer. Both spectrometers are interfaced to Nicolet 1080 minicomputers and were operated in the Fourier transform mode with quadrature detection. Typical spectral accumulation conditions were as follows: 90° pulse, 4-s pulse interval, 256–1024 scans, 2 × 8192 time domain addresses and 13888.89-Hz spectral width (6.34 T), and 2 × 4096 time domain addresses and 4504.5-Hz spectral width (2.35 T). Sample temperature was controlled with a Varian variable temperature controller. Proton decoupling at 6.34 T was effected by using a phase-modulated broad-band proton decoupler (Grutzner & Santini, 1975) at 3–4 W of power, with an effective decoupling range of about 2 ppm on either side of the center frequency. At 2.35 T proton decoupling was effected by using a noise-modulated proton decoupler with an effective decoupling range of about ±3 ppm. Line widths of selected resonances are peak widths at half-height, measured

† From the Department of Chemistry, Indiana University, Bloomington, Indiana 47405. *Received September 17, 1981.* This work was supported by National Institutes of Health Research Grant GM-19631.

* Address correspondence to the author at the Department of Chemistry, University of Iowa, Iowa City, IA 52242.

[1] Abbreviations: NMR, nuclear magnetic resonance; T, tesla, the units of magnetic field strength equal to 10^4 G; T_1, spin–lattice relaxation time; T_2, spin–spin relaxation time; NOE, nuclear Overhauser enhancement; TLC, thin-layer chromatography; CPK, Corey–Pauling–Koltun; LW, line width.

0006-2960/82/0421-3548$01.25/0

to the nearest 0.5 Hz. Spin–lattice relaxation times were determined by the fast inversion recovery method (Sass & Ziessow, 1977). Values of T_1 were calculated by a nonlinear least-squares fit to the function $I(\tau) = A - B \exp(-\tau/T_1)$ (Kowalewski et al., 1977), in which $I(\tau)$ is the intensity for a delay time τ. Integrated intensities were determined digitally with the program NTCFT supplied by Nicolet. NOE's were the ratios of intensities with continuous proton decoupling to those with the decoupler gated on during data acquisition. A delay time of $\sim 10T_1$ between data acquisitions and successive pulses was used.

Cholesteryl oleate and cholesteryl linoleate were obtained from Nu-Chek Prep., Inc., and were used without further purification. Both esters gave single spots on silica gel IB2 TLC plates (J. T. Baker Chemical Co.) with hexane–diethyl ether–glacial acetic acid (90:10:1 v/v) as the mobile phase and iodine vapor to visualize spots. When isotropic colorless liquid samples of cholesteryl oleate and cholesteryl linoleate were gradually cooled, the appearance of a bluish tint occurred at 44 and 35 °C, respectively, signaling the onset of the respective isotropic to cholesteric phase transitions. These transition temperatures agree quite well with those reported by Hamilton et al. (1977) for cholesteryl oleate (43–44 °C) and cholesteryl linoleate (34–35 °C). Spectra were taken at 6.34 T on 5 g of the respective esters in 15-mm outside diameter glass NMR tubes and at 2.35 T on 4 g of cholesteryl linoleate in 12-mm outside diameter glass NMR tubes. Before NMR spectral accumulation, the ester samples were maintained for 30 min at the experimental temperature.

Calculation of spin–spin and spin–lattice relaxation times and NOE's was performed on a CDC 6600 computer at Indiana University's Wrubel Computing Center. Plotted representations of three-dimensional surfaces were produced on a Calcomp 1037 plotter at the Wrubel Computing Center by using the three-dimensional plotting package JHVIEW.

Results and Discussion

Description of Calculational Model. Examination of a CPK space-filling model of cholesteryl myristate with the molecule in the fully extended conformation reveals that, to a good approximation, individual cholesteryl ester molecules are shaped like axially symmetric ellipses. Since the rigidty of the fused ring system of cholesteryl esters likely precludes internal reorientation of ring ^{13}C–^{1}H bonds of appreciable amplitude, the primary modes of reorientation of these bonds are the rotational diffusive motions of the entire cholesteryl ester molecule. The equations developed by Woessner (1962b) and the expressions of Doddrell et al. (1972) for a ^{13}C nucleus relaxing by dipolar interaction with ^{1}H have thus been used to calculate T_1's, line widths, and NOE's for a ^{13}C–^{1}H bond undergoing axially symmetric ellipsoidal reorientation.

Consider the depiction of a cholesteryl ester molecule in Figure 1. The Cartesian frame in the upper left-hand corner of Figure 1 is used to describe motion of the steroid ring system and hence of the ^{13}C–^{1}H bonds (dipole–dipole interaction vectors) that are constituents of the steroid rings. Motion about the z axis of the cholesteryl ester molecule is approximated as motion about the unique symmetry axis of an axially symmetric ellipse and thus has a rotational diffusion correlation time τ_{RZ}. Motions about the x and y axes are equivalent, and each has a correlation time τ_{RX}. So that the angles (θ's) for various ^{13}C–^{1}H bonds could be computed, the z axis of the cholesteryl ester molecule was taken as collinear with the C3,C13 internuclear vector. The atomic coordinates of nonhydrogen atoms of cholesteryl 17-bromoheptadecanoate (Abrahamsson & Dahlen, 1977) and the calculated positions

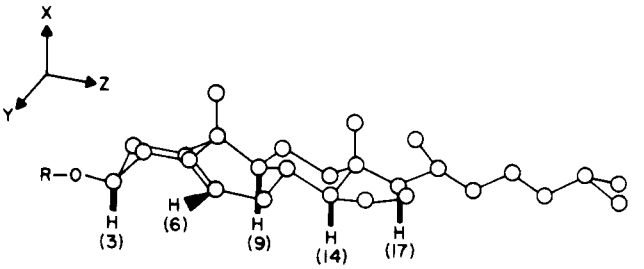

FIGURE 1: Depiction of a cholesteryl ester molecule oriented in a Cartesian coordinate frame.

of pertinent hydrogen atoms (with a C–H bond length of 1.09 Å and tetrahedral or trigonal geometry) were used to calculate the angle θ between a particular C–H bond and the chosen z axis. This procedure gives an angle θ for the C6–H bond (cf. Figure 1) of 55.7°. The angles for the other C–H bonds denoted in Figure 1 are very similar; hence θ for the C3–H bond of 73.2° is taken as representative. Taylor et al. (1981) calculated the orientation of the motional symmetry axis of cholesterol contained in bilayers of egg phosphatidylcholine from quadrupole splittings observed for deuterium labels at positions 2, 3, 4, 6, and 7 of the steroid ring system. their analysis yielded angles with respect to the symmetry axis of 79 and 56° for C3–^{2}H and C6–^{2}H, respectively, in reasonable agreement with the corresponding angles calculated herein by assuming the C3,C13 internuclear vector is the symmetry axis of cholesteryl esters. As shall be seen below, the difference in the angles of the C6–H and C3–H bonds of cholesteryl esters with respect to the (approximated) molecular symmetry axis has an important effect on the spin–spin relaxation times, and correspondingly on the line widths, of the C6 and C3 ^{13}C resonances.

Calculation of Spin–Lattice Relaxation Times, Line Widths, and NOE's. The spectral density functions of Woessner (1962b) contain r^{-6}, the ^{13}C–^{1}H internuclear distance. For methine and vinyl carbons r^{-6} will be important only for directly bonded protons. For C3–H r^{-6} was set at 1.11 Å, the C–H bond length of ethane, and for C6–H r^{-6} was set at 1.10 Å, the bond length of the vinyl C–H bonds of propene (Kuchitsu, 1972). Spin–lattice relaxation times were then calculated for C3 and C6 of cholesteryl esters over a grid of τ_{RX},τ_{RZ} pairs at magnetic field strengths of 2.35 and 6.34 T. The predicted dependences of T_1's for C3 and C6 at 6.34 T on molecular rotation correlation times are plotted as representations of three-dimensional surfaces in Figure 2.

The T_1 surfaces show that axially symmetric motion of a ^{13}C–^{1}H bond generates a dependence of T_1 on correlation times that contains a minimum contour that runs through each surface like a valley. T_1 surfaces for C3 and C6 calculated for a magnetic field of 2.35 T (not shown) are very similar in shape to those in Figure 2. However, there are important magnetic field strength effects on the calculated T_1's; over the range of correlation time pairs examined, T_1 at 6.34 T is $\geq$ T_1 at 2.35 T. In addition, there are quantitative differences between the T_1 surfaces for C3 and C6 at 6.34 T. These quantitative differences are best discussed by turning to the various transits of the T_1 surfaces shown in Figure 3. Figure 3A shows anisotropic transits for C3 and C6 that run parallel to the log τ_{RZ} axis. For these transits, log τ_{RZ} is varied at constant log τ_{RX}. The left-hand side of Figure 3A then represents highly anisotropic motion, with reorientation about the ellipse symmetry axis 1000 times faster than about either of the nonunique axes. For all pairs of correlation times, there is a marked field dependence for both C3 and C6. However, at a particular magnetic field strength, the relative value of

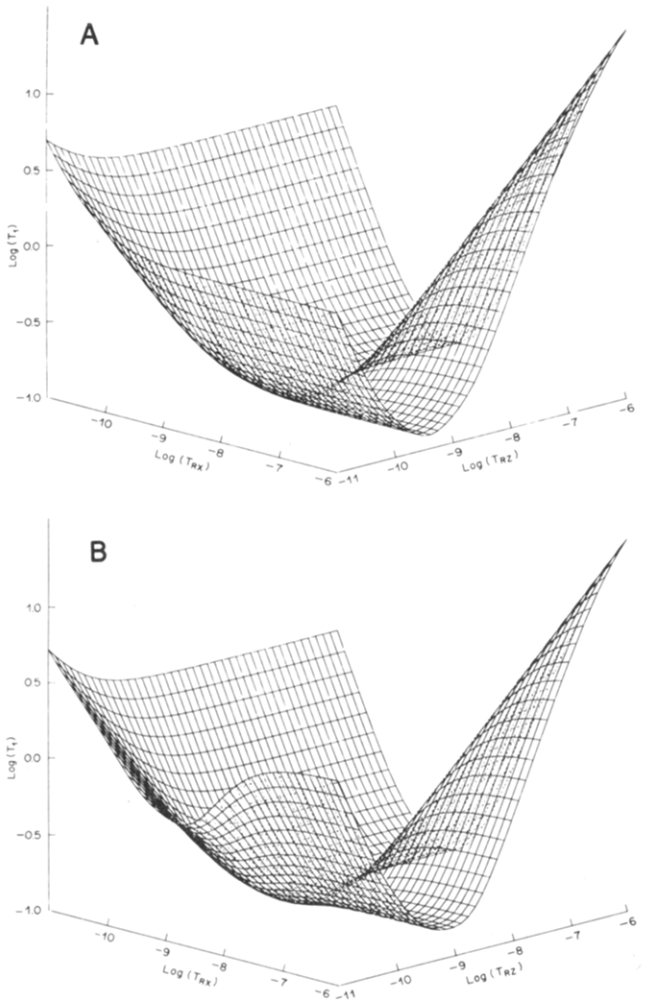

FIGURE 2: Calculated surfaces for dependence of ^{13}C spin–lattice relaxation times at 6.34 T on correlation times of rotational reorientation of an axially symmetric cholesteryl ester molecule: (A) C6 surface; (B) C3 surface.

T_1 for C6 and C3 depends on log τ_{RZ}. A crossover in T_1 occurs near the C3 minimum at $\tau_{RZ}\omega_C \approx 0.5$. The C6 minimum, which occurs at $\tau_{RZ}\omega_C \approx 0.17$, is at shorter correlation time and shorter T_1 than is that for C3. This is primarily due to the difference in the angle of the respective C–H bonds with respect to the symmetry axis (55.7° for C6–H; 73.2° for C3–H). This is underscored by the isotropic transits of Figure 3C. When motions about all three axes are equal in rate, Woessner's spectral density functions reduce to those derived by Doddrell et al. (1972) for isotropic motion, with only a single molecular motion (and nuclear) correlation time and no angular dependence. The T_1 projections of Figure 3C are similar to those of Doddrell and colleagues, with minima at $\tau_R\omega_C \approx 0.8$. That T_1 for C6 is slightly shorter than that for C3 at all correlation times is solely due to the different bond lengths chosen for the calculations (1.11 Å for C3–H; 1.10 Å for C6–H) and hence to the different r^{-6} values.

Figure 3B shows anisotropic transits of the T_1 surfaces running parallel to the log τ_{RX} axis at log $\tau_{RZ} = -7$. These transits represent motions of an oblate ellipse. In this case, the differences in projected T_1's for C3 and C6 are much less striking than for motion of a prolate ellipse (cf. Figure 3A). As shall be discussed below, the measured T_1's, line widths, and NOE's of C3 and C6 of neat cholesteryl esters are well modeled by prolate ellipsoidal reorientation.

Figure 4 shows plotted representations of three-dimensional surfaces for the dependence of C6 and C3 line widths on

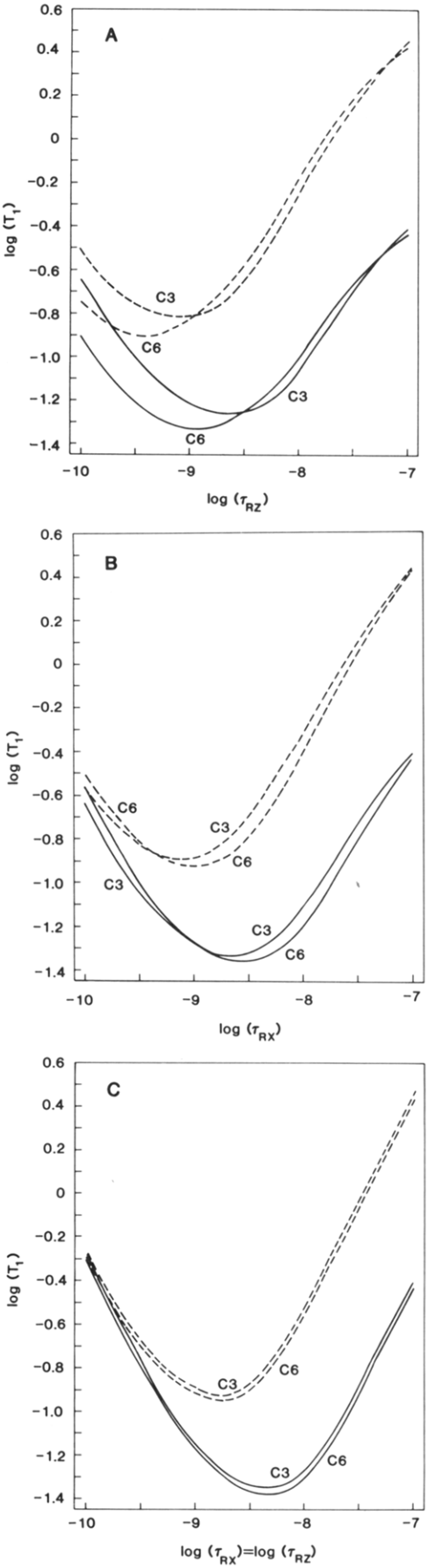

FIGURE 3: Various transits of T_1 surfaces for C3 and C6 of cholesteryl esters at 2.35 T (solid lines) and 6.34 T (broken lines): (A) anisotropic transits for prolate ellipsoidal reorientation; (B) anisotropic transits for oblate ellipsoidal reorientation; (C) isotropic transits.

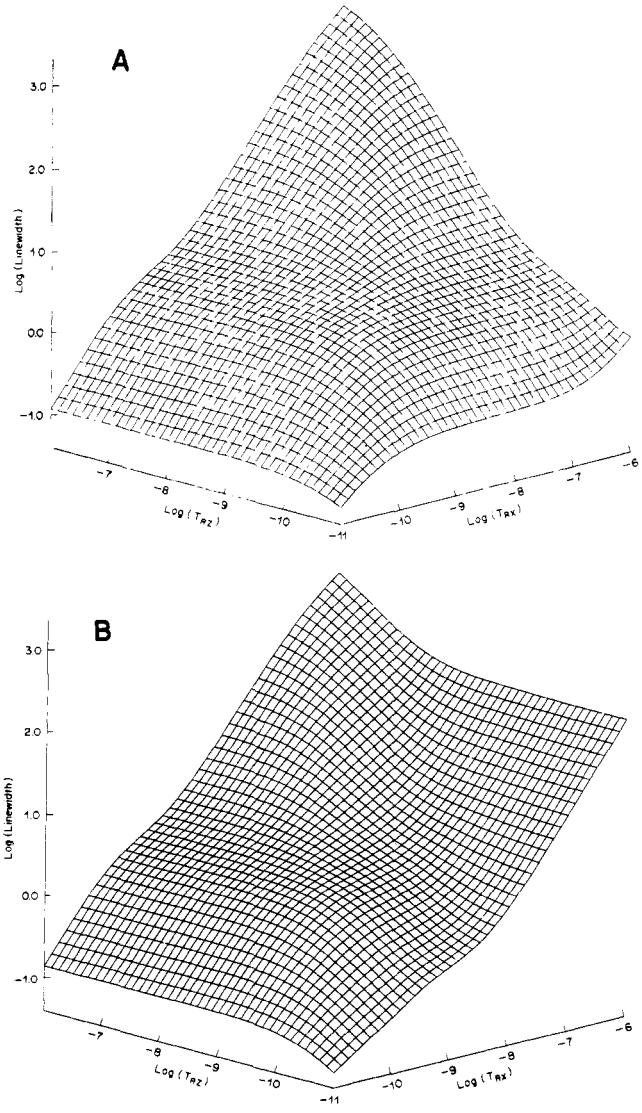

FIGURE 4: Calculated surfaces for dependence of ^{13}C line widths at 6.34 T on correlation times of rotational reorientation of an axially symmetric cholesteryl ester molecule: (A) C6 surface; (B) C3 surface.

correlation times. The projected line widths of C6 and C3 increase in a monotonic fashion from narrowest when both τ_{RX} and τ_{RZ} are short (10^{-11} s) to broadest when both correlation times are long (10^{-6} s). Also, the surfaces for C3 and C6 are very similar quantitatively except in their rightmost portions ($\tau_{RZ} \ll \tau_{RX}$); this corner of the respective surfaces is the "anisotropic corner" for prolate ellipsoidal reorientation.

Figure 5 compares various transits on the C6 and C3 surfaces at 6.34 T, as well as transits from line-width surfaces at 2.35 T (surfaces not shown). Figure 5B,C shows that, when motion is isotropic ($\tau_{RX} = \tau_{RZ}$) or is anisotropic and oblate ellipsoidal ($\tau_{RX} < \tau_{RZ}$), there is very little difference in the line widths of C3 and C6 at a particular field. The predictions of Figure 5B for the line width of C6 at 2.35 T, as well as for the C6 line-width field dependence, are similar to those of Doddrell et al. for isotropic reorientation of a ^{13}C–^{1}H bond with r = 1.09 Å. Again, this is expected since the spectral density functions of Woessner (1962b) reduce to the isotropic case when $\tau_{RX} = \tau_{RZ}$.

Figure 5A predicts that, when motion is highly anisotropic ($\tau_{RZ} \ll \tau_{RX}$) and prolate ellipsoidal as expected for cholesteryl esters, the C6 resonance will be *significantly narrower* than the C3 resonance. This is due to the "magic angle" effect, arising from the dependence of Woessner's spectral density

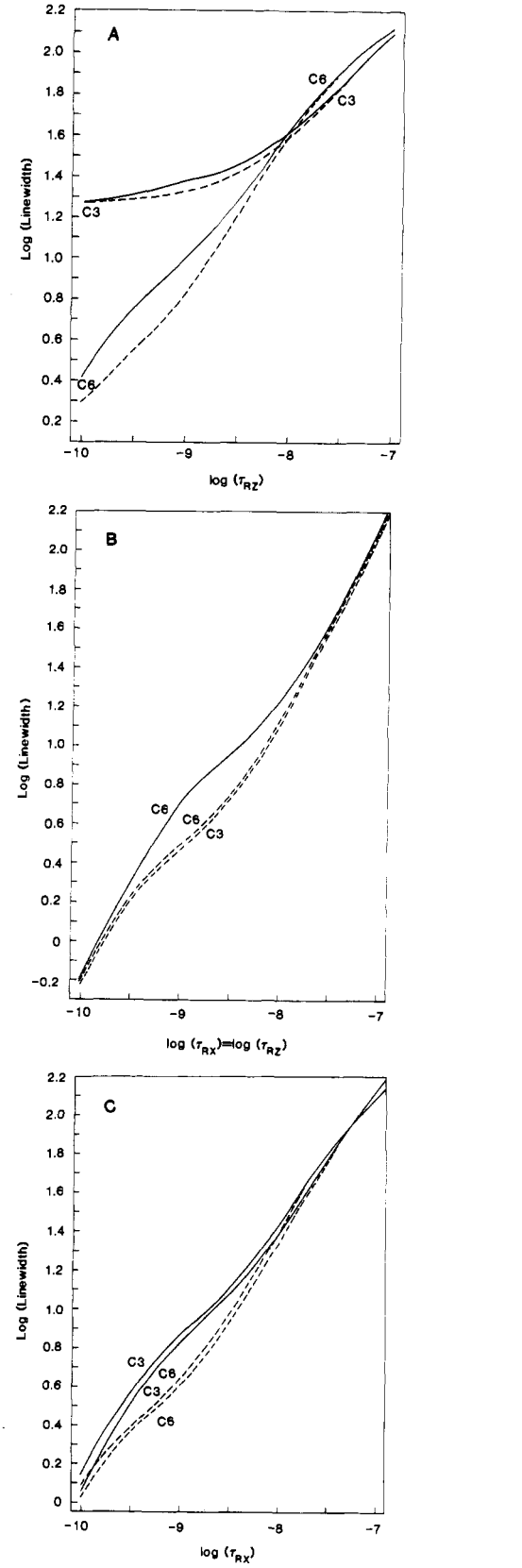

FIGURE 5: Various transits of line-width surfaces for C3 and C6 of cholesteryl esters at 2.35 T (solid lines) and 6.34 T (broken lines): (A) anisotropic transits for prolate ellipsoidal reorientation; (B) isotropic transits (the line for C3 at 2.35 T, which like that at 6.34 T runs closely parallel to the C6 line, has been omitted for clarity); (C) anisotropic transits for oblate ellipsoidal reorientation.

functions on the angle θ between the ^{13}C–^{1}H bond and the symmetry axis of the ellipse. When a ^{13}C–^{1}H bond lies at the magic angle with respect to the symmetry axis of the ellipse,

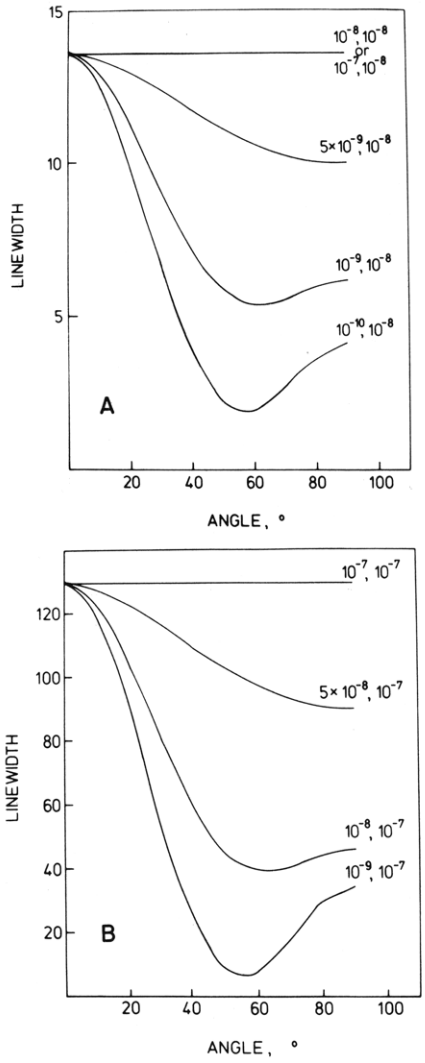

FIGURE 6: Dependence of calculated ^{13}C line width at 6.34 T on angle of inclination, θ, of the ^{13}C–^{1}H internuclear vector with respect to the symmetry axis of the cholesteryl ester molecule. For these calculations, the bond length is $r = 1.10$ Å. (A) $\tau_{RX} = 10^{-8}$ s and τ_{RZ} is variable as indicated; (B) $\tau_{RX} = 10^{-7}$ s and τ_{RZ} is variable as indicated.

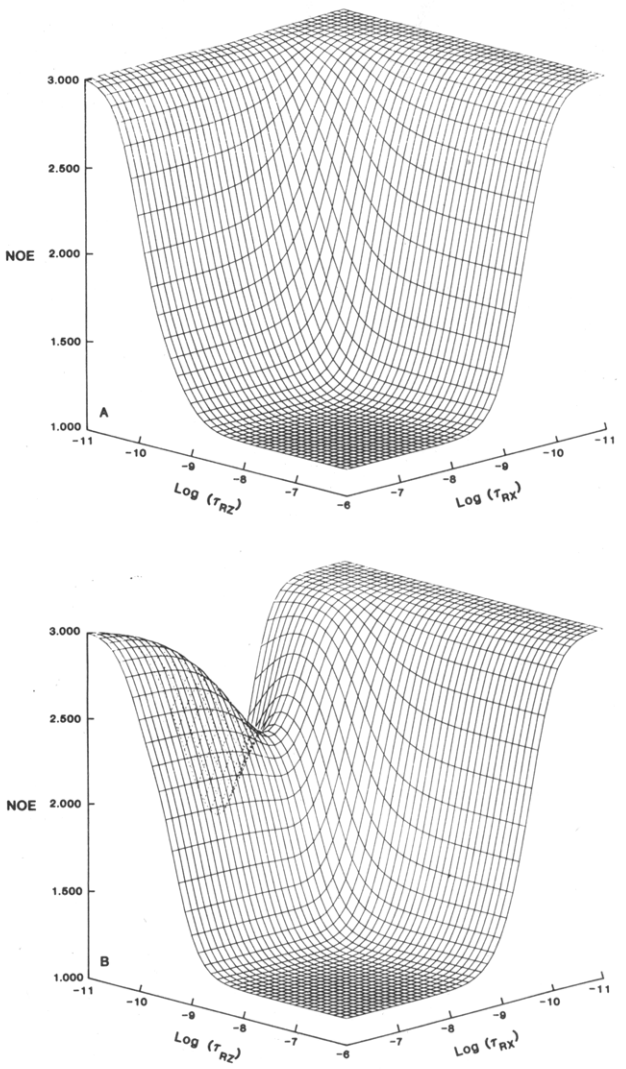

FIGURE 7: Calculated surfaces for dependence of ^{13}C NOE's of (A) C6 and (B) C3 on correlation times of rotational reorientation of an axially symmetric cholesteryl ester molecule.

the ^{13}C–^{1}H dipole–dipole interaction is minimal. The magic angle plots of Figure 6 illustrate this point. When motion is highly anisotropic and prolate ellipsoidal, the C6 resonance is significantly narrower than that of C3 since the C6–H bond is inclined at $\theta = 55.7°$ (near the plotted minimum) with respect to the symmetry axis, but the C3–H bond is inclined at $\theta = 73.2°$.

Brainard and Szabo have formulated a model for the motion of cholesterol in phospholipid vesicles, in which motion about the cholesterol symmetry axis (z axis of Figure 1) is rapid but spatially unrestricted and motions about the x and y axes are slower and restricted, so that motion occurs in a cone. Their model, which is geometrically distinct from that discussed here for cholesteryl esters, predicts that the C6 resonance is significantly narrower than those of C3 and C9 because of the magic angle effect. However, Brainard and Szabo's model also predicts a significant magic angle effect when motions about the x and y axes are spatially unrestricted and motion is highly anisotropic since, as they state, their spectral density functions reduce exactly to those of Woessner (1962b).

Surfaces for the dependence of the NOE's of the C3 and C6 resonances of cholesteryl esters were also calculated and are displayed in Figure 7. For C6, the NOE varies monotonically from 1.153 when both τ_{RX} and τ_{RZ} are long (10^{-6} s) to 2.988 when either correlation time is short (10^{-11} s). This is the same range predicted for the NOE of a ^{13}C nucleus reorienting isotropically (Doddrell et al., 1972). The C3 surface gives calculated NOE's that are numerically similar to those of C6 except in the leftmost portion of the surface. The col in the C3 surface comes when $\tau_{RZ} \ll \tau_{RX}$, i.e., when motion is that of a prolate ellipse. Since the C6 and C3 line widths of cholesteryl esters require that $\tau_{RZ} \ll \tau_{RX}$, NOE predictions will come from the left-hand portions of the respective surfaces.

Quantitative Modeling of Anisotropic Motion of Cholesteryl Esters. ^{13}C NMR spectra of neat cholesteryl linoleate at 2.35 T and neat cholesteryl oleate and cholesteryl linoleate at 6.34 T were acquired at various temperatures at and above the temperatures of the respective isotropic to cholesteric phase transitions. Spectra of cholesteryl linoleate taken at 6.34 T at three temperatures are shown in Figure 8. These spectra are similar to those of Hamilton et al. (1977) taken at 2.35 T, save that greater resolution in the 0–50-ppm region, consisting primarily of resonances from the linoleoyl chain and the steroid C17 side chain, is realized at high field. Like the spectra of Hamilton et al. (1977), the spectra of cholesteryl linoleate in Figure 8 depend markedly on temperature. Of particular interest are the indicated resonances contributed by carbons 3, 5, 6, 9, and 14,17 of the steroid fused ring system.

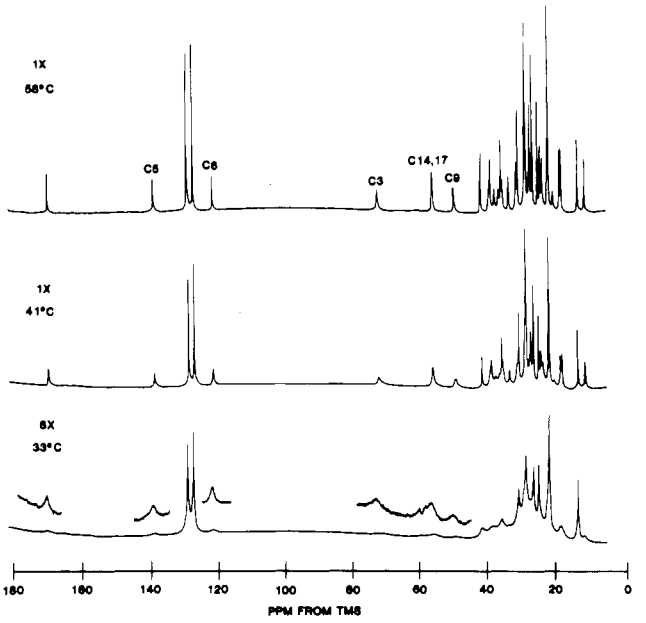

FIGURE 8: Natural abundance ^{13}C Fourier transform NMR spectra at 6.34 T of neat cholesteryl linoleate. An additional 8-fold scale expansion was used to produce the insets of the spectrum at 33 °C.

Table I: Line Widths at 6.34 T and Projected Correlation Times for Cholesteryl Esters

temp (°C)[a]	LW (Hz)[b] C3	LW (Hz)[b] C6	C3/C6 ratio	calcd values[c] τ_{RX} (s)	calcd values[c] τ_{RZ} (s)	calcd values[c] τ_{RX}/τ_{RZ}
Cholesteryl Linoleate						
33	175	81	2.16	8.0×10^{-7}	1.5×10^{-8}	53
36	70.5	32.5	2.17	3.0×10^{-7}	6.0×10^{-9}	50
40	47	27	1.74	2.0×10^{-7}	5.0×10^{-9}	40
42	34.5	17.5	1.97	1.5×10^{-7}	3.5×10^{-9}	43
46	25	12	2.08	1.1×10^{-7}	2.1×10^{-9}	52
50	20	10.5	1.90	8.2×10^{-8}	1.8×10^{-9}	46
52	16	9	1.78	6.3×10^{-8}	1.5×10^{-9}	42
57.5	10	5	2.00	4.0×10^{-8}	6.4×10^{-10}	62
Cholesteryl Oleate						
45.5	53	27	1.96	2.3×10^{-7}	5.0×10^{-9}	46
46.5	57	22	2.59	2.6×10^{-7}	4.0×10^{-9}	65
53.5	30	13	2.31	1.3×10^{-7}	2.3×10^{-9}	57
58	17	8	2.12	7×10^{-8}	1.3×10^{-9}	54
60	15	7.5	2.00	6×10^{-8}	1.2×10^{-9}	50
65.5	11	5.5	2.00	4.5×10^{-8}	7.5×10^{-10}	60

[a] Uncertainty in temperature is ±1 °C. [b] Measured line widths contain a contribution from magnetic field drift and inhomogeneity. 3 Hz has thus been subtracted from line widths to account for these contributions. Precision of line widths is ±10%, save that for C3 of cholesteryl linoleate at 33 °C, which is ±20%. [c] Uncertainties in τ_{RX} and τ_{RZ} arising from line-width uncertainties are ±10–15%.

These resonances broaden progressively as the temperature is lowered and at the isotropic to cholesteric transition are virtually broadened into the base line. The spectrum of Figure 8 at 33 °C shows residual contribution from steroid ring resonances. At this temperature, cholesteryl linoleate is in a smectic mesophase (Hamilton et al., 1977). However, the temperature I report for this spectrum is the average temperature of the sample just after removal from the magnet. A thermal gradient across the sample volume of 2–3 °C was consistently observed at all temperatures in experiments conducted at high field. For this reason, the spectrum at 33 °C consists of sharper lines than that of Hamilton et al. at 2.35 T, with the residual sharp component presumably contributed by cholesteryl linoleate in the warmer part of the

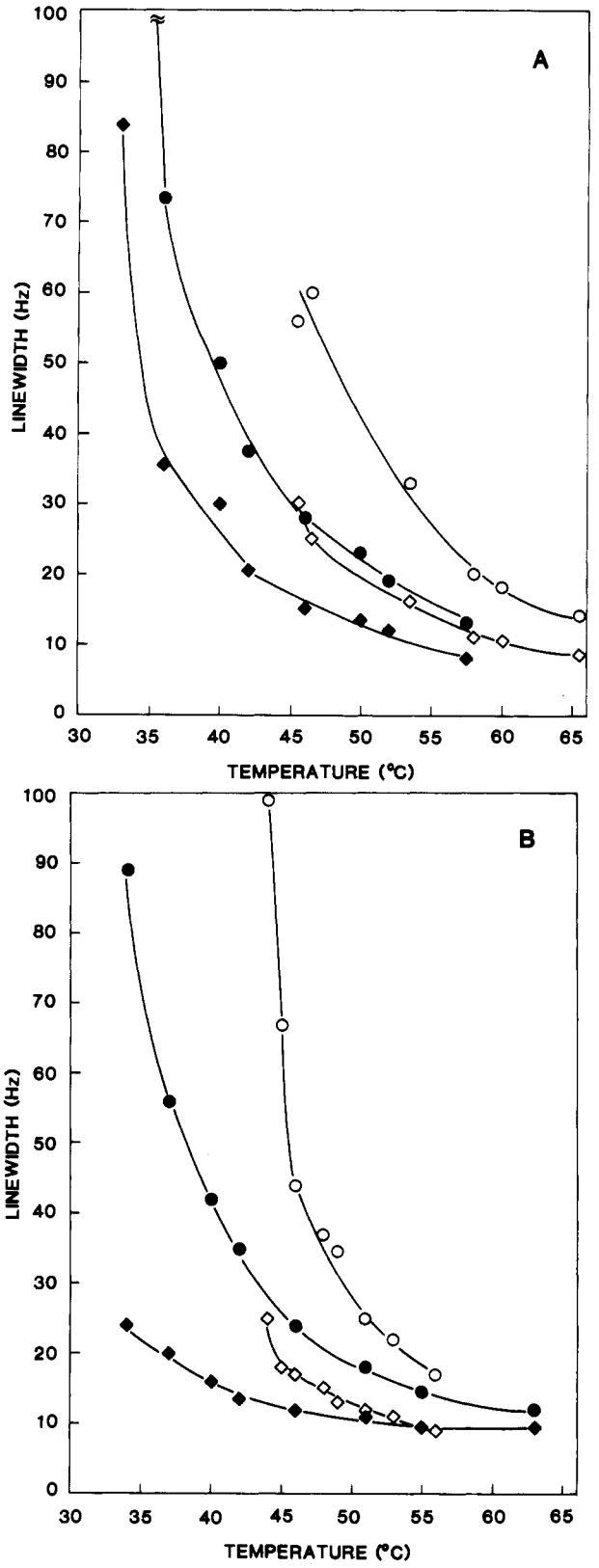

FIGURE 9: Dependence of line widths of C3 and C6 of cholesteryl linoleate and cholesteryl oleate on temperature at (A) 6.34 and (B) 2.35 T: (○ and ◇) C3 and C6, respectively, of cholesteryl oleate; (● and ◆) C3 and C6, respectively, of cholesteryl linoleate.

sample. The spectra of cholesteryl linoleate determined at low field (2.35 T, spectra not shown) were acquired on the same NMR spectrometer as used by Hamilton et al. and agree with heir spectra in detail. Temperature control at 2.35 T was much better than at 6.34 T, and consequently thermal gra-

Table II: Line Widths at 2.35 T and Projected Correlation Times for Cholesteryl Esters

temp (°C)[a]	LW (Hz)[b] C3	LW (Hz)[b] C6	C3/C6 ratio	calcd values[c] τ_{RX} (s)	calcd values[c] τ_{RZ} (s)	calcd values[c] τ_{RX}/τ_{RZ}
			Cholesteryl Linoleate			
34	89	24	3.71	4.3×10^{-7}	3.8×10^{-9}	113
37	56	20	2.80	2.5×10^{-7}	3.0×10^{-9}	83
40	42	16	2.62	1.9×10^{-7}	2.2×10^{-9}	86
42	35	13.5	2.59	1.5×10^{-7}	1.7×10^{-9}	88
46	24	12	2.00	9.5×10^{-8}	1.5×10^{-9}	63
51	18	11	1.64	6.0×10^{-8}	1.5×10^{-9}	40
55	14.5	9.5	1.53	3.8×10^{-8}	9.2×10^{-10}	41
63	12	9.5	1.26	3.3×10^{-8}	9.6×10^{-10}	34
			Cholesteryl Oleate[d]			
44	99	25	3.96	5.0×10^{-7}	3.9×10^{-9}	128
45	67	18	3.72	3.3×10^{-7}	2.6×10^{-9}	127
46	44	17	2.59	2.0×10^{-7}	2.5×10^{-9}	80
48	37	15	2.47	1.6×10^{-7}	2.0×10^{-9}	80
49	35	13	2.69	1.6×10^{-7}	1.5×10^{-9}	107
51	25	12	2.08	1.0×10^{-7}	1.5×10^{-9}	67
53	22	11	2.00	8.5×10^{-8}	1.3×10^{-9}	65
56	17	9	1.89	6.5×10^{-8}	8×10^{-10}	81

[a] Uncertainty in temperature is ±0.5 °C. [b] Precision in line widths is considered ±10%. [c] Uncertainties in τ_{RX} and τ_{RZ} arising from line-width uncertainties are ±10–15%. [d] Line widths for cholesteryl oleate are from Hamilton et al. (1977).

dients across the sample were never detected at low field. The temperature dependences of the line widths of C3 and C6 of cholesteryl oleate and cholesteryl linoleate at low and high fields are plotted in Figure 9. These plots show that at both fields the line widths of steroid ring carbon resonances are sensitive indicators of the approach of the isotropic to cholesteric phase transition, as suggested by Hamilton et al. (1977).

Since the C6 and C3 resonances of isotropic phase cholesteryl linoleate and cholesteryl oleate progressively broaden as the temperature is lowered [accompanied by an increase in the macroscopic viscosity (Hamilton et al., 1977)], the line-width surfaces of Figure 4 were used to generate values for the rotational diffusion correlation times of the steroid fused ring system. This can be done because, even though a particular measured C3 or C6 line width and its estimated uncertainty give a large number of τ_{RX},τ_{RZ} solutions corresponding to projection of the appropriate line-width contour onto the log τ_{RX},log τ_{RZ} plane, the *overlap* of solutions from the C3 surface and the C6 surface yields a small range of acceptable τ_{RX},τ_{RZ} pairs. Correlation times calculated in this way are listed in Tables I and II; the ratio of correlation times in the rightmost columns of Tables I and II are the calculated rotational anisotropies of the respective esters.

The anisotropy of steroid ring motion calculated from line widths in Table II generally increases as the temperature is lowered. This trend indicates that as the isotropic to cholesteric phase transition is approached a pretransition ordering of cholesteryl esters occurs; i.e., motion about the symmetry axis increases in correlation time at a slower rate than does that about the x and y axes (cf. Figure 1). No such trend in steroid ring rotational anisotropy is evidenced by correlation times calculated from line widths measured at 6.34 T and listed in Table I. However, this is likely due to the thermal gradient across the sample volume that was discussed above. A thermal gradient would give rise to a measured line width that is a

Table III: Comparison of Measured and Calculated NOE's of Cholesteryl Esters

ester	field (T)	temp (°C)[a]	measured NOE[b] C6	measured NOE[b] C3	calcd NOE C6	calcd NOE C3
cholesteryl oleate	6.34	47	1.20 ± 0.06	1.45 ± 0.04	1.17 ± 0.01[c]	1.17 ± 0.01[c]
					1.20 ± 0.01[d]	1.22 ± 0.01[d]
		56	1.37 ± 0.03	1.54 ± 0.05	1.27 ± 0.02[c]	1.34 ± 0.04[c]
					1.35 ± 0.03[d]	1.49 ± 0.06[d]
cholesteryl linoleate	6.34	43	1.46 ± 0.06	1.6 ± 0.1	1.17 ± 0.01[c]	1.18 ± 0.01[c]
					1.23 ± 0.03[d]	1.28 ± 0.06[d]
cholesteryl oleate	2.35	48	1.7 ± 0.1	1.6 ± 0.1	1.24 ± 0.02[c]	1.28 ± 0.04[c]
					1.4 ± 0.1[d]	1.5 ± 0.1[d]
		56	1.9 ± 0.1	1.71 ± 0.07	1.52 ± 0.04[c]	1.79 ± 0.08[c]
					1.67 ± 0.06[d]	2.03 ± 0.07[d]

[a] Uncertainty in temperature is ±1–2 °C. [b] NOE's were measured as the ratio of the average integrated intensity from three spectra, each with continuous and with gated proton decoupling. Uncertainty in NOE is the standard error, calculated from the standard errors of the mean of the integrated intensities from which the NOE is calculated. [c] NOE's were calculated from τ_{RX},τ_{RZ} pairs listed in Table I; uncertainties were estimated from uncertainites in τ values. [d] Same as footnote *c* but with τ values from Table II.

Table IV: Spin-Lattice Relaxation Times

ester	magnetic field strength (T)	temp (°C)[a]	measured T_1 (s)[b] C3	measured T_1 (s)[b] C6	calcd T_1 (s)[c] C3	calcd T_1 (s)[c] C6
cholesteryl oleate	2.35	47.5	0.070	0.057	0.056	0.050
		50	0.074	0.060	0.058	0.048
		59	0.085	0.062	0.058	0.047
	6.34	64	0.28	0.17	0.15	0.13
cholesteryl linoleate	2.35	46	0.088	0.061	0.056[d]	0.050[d]
					0.058	0.048
	6.34	46	0.21	0.16	0.18	0.20
					0.16[e]	0.17[e]

[a] Uncertainty in temperature is ±1 °C. [b] Estimated uncertainty of measured spin-lattice relaxation times is ±10%, save for cholesteryl oleate at 6.34 T, where uncertainty is ±20%. T_1's of cholesteryl oleate at 2.35 T are from Hamilton et al. (1977). [c] Except as noted, T_1's were calculated from τ_{RX},τ_{RZ} values listed in Tables I and II by using line widths measured at the same field as that where T_1's were measured. Where necessary, τ's used for calculation of T_1's were determined by linear interpolation. [d] Calculated from τ_{RX},τ_{RZ} values listed in Table I at 46 °C. [e] Calculated from τ_{RX},τ_{RZ} values listed in Table II at 46 °C.

composite of overlapping line widths from cholesteryl esters experiencing different temperatures. This situation would be especially prominent at temperatures approaching the isotropic to cholestric transition, where the C3 and C6 lines are rapidly broadening (cf. Figure 9). Nonetheless, one consistent prediction comes from the calculated correlation times of Tables I and II: the rotational diffusive motion of isotropic phase cholesteryl esters is highly anisotropic.

Another explanation for the different trends in calculated anisotropy at low and high fields is that chemical shift anisotropy (CSA) contributes to spin–spin relaxation, and hence line width, of the C6 resonances. However, the NOE's for C3 and C6 of cholesteryl oleate (Table III) indicate that such is probably not the case. The reasonable agreement of measured and calculated NOE's at both fields suggests that NOE's of isotropic phase cholesteryl esters are well modeled by Woessner's (1962b) spectral density functions when the motion is prolate ellipsoidal. Especially pertinent are the C6 NOE's at 6.34 T, where the agreement between calculation and measurement is quite good. Were CSA an important relaxation mechanism for C6 under these conditions, the NOE of C6 should be closer to 1.0 than the predicted NOE, since there is no NOE for CSA relaxation. However, in each instance, the measured NOE is at least as large as the calculated NOE.

Hamilton et al. (1977) also suggested from line widths measured at 2.35 T that motion of the steroid rings of cholesteryl esters is anisotropic, though they did not make a quantitative assessment of the anisotropy. The nature of the anisotropic motion that they describe is quite different than that detailed herein. They ascribe differences in the line widths of C3 and C6 to faster motion about the y axis than about the x axis of Figure 1; in their model, motion about the z axis of Figure 1 reorients both C3–H and C6–H and thus does not contribute to line-width differences. However, the calculations detailed herein suggest that the narrower C6 resonance vs. that of C3 is due to faster motion about the symmetry axis (z axis) of the cholesteryl ester molecule than about the two orthogonal, nonunique axes and to the inclination of the C6–H internuclear vector near the magic angle with respect to the symmetry axis (cf. Figures 5 and 6). In the axially symmetric diffusion model described by Woessner's (1962b) spectral density functions, motions about the x and y axes have equal correlation times and do not contribute, per se, to the different C3 and C6 line widths.

Another test of the rotational motion model discussed in this paper for cholesteryl esters is the ability of the model to predict both the magnitude and the field dependence of measured T_1's for C3 and C6 by using correlation times generated from line-width measurements and the T_1 surfaces of Figure 2. Table IV makes such comparisons of measured and projected T_1's. The agreement between calculation and experiment is quite good, especially when one considers the experimental errors in measured T_1's and the uncertainties in projected T_1's arising from uncertainties in correlation times (±10–15%; cf. Tables I and II). Only in a few cases are projected T_1's different than measured T_1's by more than the sum of the estimated uncertainties.

The model suggested in this presentation for the molecular dynamics of the cholesteryl ester steroid ring system contains a number of approximations. The most important is that cholesteryl esters are shaped like axially symmetric ellipses. From this assumption others follow, including the placement of the symmetry axis and the consequent calculation of the angles of the C6–H and C3–H internuclear vectors with respect to the symmetry axis. Finally, the bond lengths for C3–H and C6–H were taken from gas-phase electron diffraction data of representative molecules (Kuchitsu, 1972), as outlined earlier. Considering these various assumptions, the agreement between measured and calculated T_1's and NOE's is reasonable. This agreement provides support for the internal, quantitative consistency of the model discussed herein for cholesteryl ester rotational dynamics.

Acknowledgments

I thank Drs. Jim Brainard, Paulus Kroon, and E. H. Cordes for discussion on and critical review of the manuscript and George Pauly for programming advice on the use of the three-dimensional plotting package JHVIEW. I also express my appreciation to Rose Alden for her expert technical assistance in the preparation of the manuscript.

References

Abrahamsson, S., & Dahlen, B. (1977) *Chem. Phys. Lipids 20*, 43–56.

Allerhand, A. (1970) *J. Chem. Phys. 52*, 3596–3599.

Allerhand, A., Doddrell, D., & Komoroski, R. (1971) *J. Chem. Phys. 55*, 189–198.

Brainard, J. R., & Szabo, A. (1981) *Biochemistry 20*, 4618–4628.

Doddrell, D., Glushko, V., & Allerhand, A. (1972) *J. Chem. Phys. 56*, 3683–3689.

Gent, M. P. N., & Prestegard, J. H. (1977) *J. Magn. Reson. 25*, 243–262.

Grutzner, J. B., & Santini, R. E. (1975) *J. Magn. Reson. 19*, 173–187.

Hamilton, J. A., Oppenheimer, N., & Cordes, E. H. (1977) *J. Biol. Chem. 252*, 8071–8080.

Kowalewski, J., Levy, G. C., Johnson, L. F., & Palmer, L. (1977) *J. Magn. Reson. 26*, 533–536.

Kroon, P. A., Quinn, D. M., & Cordes, E. H. (1982) *Biochemistry 21*, 2745–2753.

Kuchitsu, K. (1972) in *MTP International Review of Science: Physical Chemistry, Series One* (Buckingham, A. D., Consultant Ed., & Allen, G., Vol. Ed.) Vol. 2, Chapter 6, University Park Press, Baltimore, MD.

Sass, M., & Ziessow, D. (1977) *J. Magn. Reson. 25*, 263–276.

Sears, B., Deckelbaum, R. J., Janiak, M. J., Shipley, G. G., & Small, D. M. (1976) *Biochemistry 15*, 4151–4157.

Tancrede, P., Deslauriers, R., McGregor, W. H., Ralston, E., Sarantakis, D., Somorjai, R. L., & Smith, I. C. P. (1978) *Biochemistry 17*, 2905–2914.

Taylor, M. G., Akiyama, T., & Smith, I. C. P. (1981) *Chem. Phys. Lipids 29*, 327–339.

Wittebort, R. J., & Szabo, A. (1978) *J Chem. Phys. 64*, 1722–1736.

Woessner, D. E. (1962a) *J. Chem. Phys. 36*, 1–4.

Woessner, D. E. (1962b) *J. Chem. Phys. 37*, 647–654.

Yeagle, P. L. (1981) *Biochim. Biophys. Acta 640*, 263–273.